

Identification of fullerene-like CdSe nanoparticles from optical spectroscopy calculations

Silvana Botti^{1,2} and Miguel A. L. Marques^{2,3}

¹Laboratoire des Solides Irradiés, CNRS-CEA-École Polytechnique, 91128 Palaiseau, France

²European Theoretical Spectroscopy Facility (ETSF)

³Centro de Física Computacional, Departamento de Física da Universidade de Coimbra, Rua Larga, 3004-516 Coimbra, Portugal

(Received 18 May 2006; revised manuscript received 24 July 2006; published 9 January 2007)

Semiconducting nanoparticles are the building blocks of optical nanodevices as their electronic states, and therefore light absorption and emission, can be controlled by modifying their size and shape. CdSe is perhaps the most studied of these nanoparticles, due to the efficiency of its synthesis, the high quality of the resulting samples, and the fact that the optical gap is in the visible range. In this article, we study light absorption of CdSe nanostructures with sizes up to 1.5 nm within density functional theory. We study both bulk fragments with wurtzite symmetry and fullerene-like core-cage structures. The comparison with recent experimental optical spectra allows us to confirm the synthesis of these fullerene-like CdSe clusters.

DOI: [10.1103/PhysRevB.75.035311](https://doi.org/10.1103/PhysRevB.75.035311)

PACS number(s): 78.67.Bf, 64.70.Nd, 71.15.Mb

I. INTRODUCTION

For the past years, semiconductor quantum dots have attracted large interest from the community due to the peculiar role played by quantum confinement¹ and the consequent potential for size-tunable nanodevices. High-quality colloidal nanoparticles can now be routinely synthesized with a remarkably narrow size distribution (even lower than 5%),² and have already proved to be excellent components for a variety of applications in opto-electronics (i.e., light-emitting diodes,³ optically pumped lasers,⁴ photovoltaic cells),⁵ in telecommunications,⁶ and in biomedicine as chemical markers.⁷ Among the colloidal nanocrystals, CdSe is perhaps the most studied, due to the efficiency of its synthesis, the high quality of the resulting samples, and the fact that the optical gap is in the visible range. In most experimental setups, CdSe nanoparticles are formed by kinetically controlled precipitation, and are terminated with capping organic ligands, like, e.g., the trioctyl phosphine oxide (TOPO) molecule, which provide stabilization of the otherwise reactive dangling orbitals at the surface.²

The understanding of the atomic arrangement and surface deformation of CdSe clusters is quite important. In fact, strong reconstructions imply necessarily important modifications of the electronic states, and consequently of the size-dependent optical properties at the basis of all technological applications. For ligand-terminated CdSe clusters, both transmission electron microscopy data,^{2,8} molecular dynamics simulations,⁹ and *ab initio* structural relaxation¹⁰ agree on predicting an atomic arrangement of the inner Cd and Se atoms analogous to the one in the wurtzite CdSe crystal. The extent to which the cluster surface retains the crystal geometry is more controversial as the surface cannot be easily resolved experimentally. Generally, if the surface is properly passivated, the reconstruction is assumed to be small and limited to the outermost layer (and eventually the layer just beneath it), which is in agreement with molecular dynamics simulations.⁹ Pudzer *et al.*¹⁰ have predicted for clusters with diameters up to 1.5 nm a strong surface reconstruction, remarkably similar in vacuum and in the presence of passivating ligands.

Recently, the synthesis and probable identification of highly stable (CdSe)₃₃ and (CdSe)₃₄ nanoparticles grown in a solution of toluene has been reported.^{11,12} The experimental absorption spectra of these nanoparticles at low temperature show sharp peaks, similar to the ones that characterize TOPO-capped clusters of the same size.² However, the surfactant molecules employed in the synthesis process are, in this case, removed by laser vaporization. Furthermore, an x-ray analysis indicates that the coordination number of Se is between 3 (the coordination of a fullerene) and 4 (the coordination of the bulk crystal). In view of this, and in absence of direct structural data, the nonpassivated compound nanoparticles are predicted to have a core-cage structure, composed by a puckered fullerene-like (CdSe)₂₈ cage accommodating a (CdSe)_n ($n=5,6$) wurtzite unit inside.

The core-cage structures proposed by Kasuya *et al.*¹¹ are significantly different from all previous bulk-derived arrangements. This geometry is proved to be particularly stable by first-principle total energy calculations.¹¹ However, up to now no definitive proof has been given for the identification of the highly stable observed nanoparticles with the fullerene-like structures.

In this work we address the problem of the identification of CdSe nanoparticles through the comparison between measured¹¹ and simulated optical spectra. In fact, as the electronic states are strongly modified by changes of size and shape, absorption (or emission) peaks are sensitive to such changes as well. Optical spectroscopy can thus be a powerful tool (especially if it can be combined with other spectroscopic techniques) to probe the atomic arrangement of synthesized nanoparticles.

The remainder of this article is organized as follows. In Sec. II we discuss the structural relaxation performed within density functional theory (DFT) for a selection of fragments with wurtzite symmetry and fullerene-like core-cage aggregates. In Sec. III we present calculations of the Kohn-Sham highest occupied molecular orbital–lowest unoccupied molecular orbital (HOMO-LUMO) gaps and the absorption spectra for the optimized geometries, comparing our results with available experimental data. Finally, in Sec. IV we draw our conclusions concerning the identification of the CdSe core-cage structures.

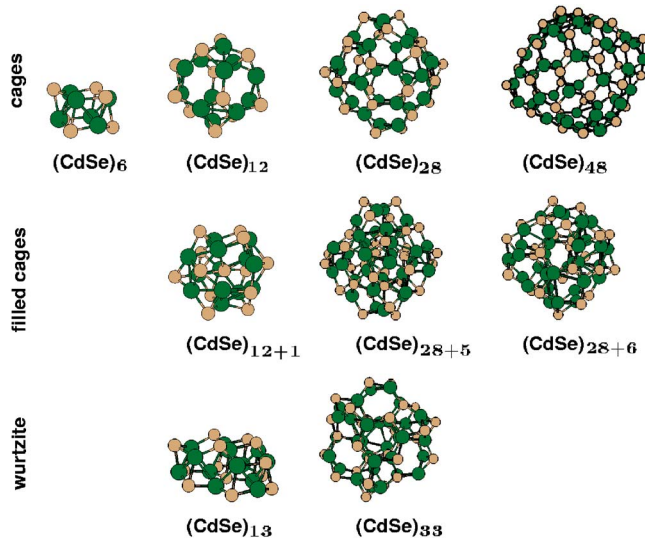


FIG. 1. (Color online) Relaxed cages, filled cages, and wurtzite structures of $(\text{CdSe})_n$. Cd atoms are in green and Se atoms are in beige.

II. GROUND-STATE CALCULATIONS

The atomic positions of our CdSe nanoparticles were obtained by geometry optimization within DFT,¹³ using norm-conserving pseudopotentials¹⁴ and the local density approximation (LDA) for the exchange-correlation potential.¹⁵ For all calculations presented here we used two Cd ($5s^2$) and six Se ($4s^2 4p^4$) valence electrons. We verified that using a pseudopotential with 18 valence electrons for Cd did not change significantly the relaxed bond lengths and angles.

We considered initial candidate structures with different sizes ranging up to about 1.5 nm. To build up these atomic arrangements we started from three different kinds of ideal geometries: (i) bulk fragments cut into the infinite wurtzite crystal, (ii) octahedral fullerene-like cages made of four- and six-membered rings, and (iii) the core-cage structures of Ref. 11, composed of puckered CdSe fullerene-type cages which include $(\text{CdSe})_n$ wurtzite units of adequate size to form a three-dimensional network. We assume that the Cd-Se distance before structural relaxation is the distance in the CdSe wurtzite crystal, calculated within DFT in the same approximations used for the nanoparticles:¹³ its value (0.257 nm) compares well with the experimental value (0.263 nm).

Atomic arrangements after optimization are depicted in Fig. 1. All clusters suffer contraction upon geometry minimization. For example, $(\text{CdSe})_{33,34}$ clusters experience a size reduction of about 1–1.5%, in agreement with the x-ray analysis of Ref. 11. However, as the relaxation affects mainly the outermost atoms, the overall effect is more pronounced in smaller structures, where the average Cd-Se distance decreases up to 4%. This contraction does not conserve the overall shape, as Cd atoms are pulled inside the cluster and Se atoms are puckered out. As a consequence, Cd-Cd average distances can be reduced by 30%, while Se-Se distances remain essentially unvaried. This is clearly visible in Fig. 2, where the relaxed distance of Cd (circles) and Se (diamonds) atoms from the center of the cluster is plotted for $(\text{CdSe})_{33,34}$

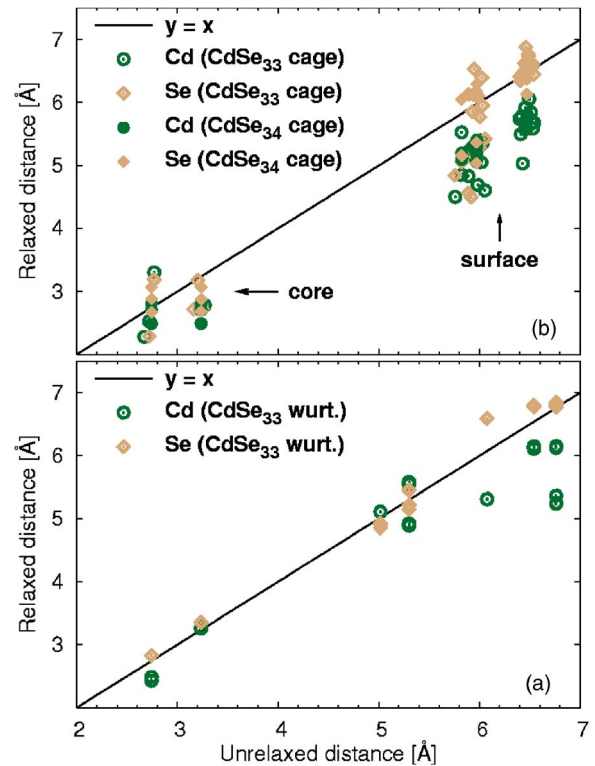


FIG. 2. (Color online) Distance of Cd atoms (circles) and Se atoms (diamonds) from the center of the cluster after geometry optimization, as a function of their distance before optimization. An atom that lies on the straight line $y=x$ has not changed its position. In panel (a) results of the analysis for $(\text{CdSe})_{33,34}$ core-cage clusters, in panel (b) for the $(\text{CdSe})_{33}$ wurtzite cluster.

clusters as a function of their distance before relaxation. If the atoms remained in their initial position, all datapoints would fall on the straight line $y=x$. The fact that most Cd atoms lie below the line, while most Se atoms are above it, shows that in our simulation Cd atoms prefer to move inward and Se atoms outward. That puckering happens independently of the cluster size and it is in agreement with previous calculations.^{10,11}

All wurtzite fragments get significantly distorted upon relaxation and break their original symmetry. In agreement with the findings of Pudzer *et al.*,¹⁰ the strong modification of bond lengths and angles concerns essentially the surface layer. In particular, we can see in Fig. 2(a) that the wurtzite-type $(\text{CdSe})_{33}$ is already large enough to conserve a bulk-like crystalline core. In fact, the spread of the points from the straight line is pronounced only for the external shell of atoms. The calculated overall contraction of the cluster is consistent with experimental data.¹⁶ Also the empty cages [$(\text{CdSe})_{12}$, $(\text{CdSe})_{28}$, and $(\text{CdSe})_{48}$] get puckered, but conserve their overall shape. Their binding energies are smaller by 0.1–0.2 eV with respect to the binding energies of the corresponding filled cages [see Fig. 3(b)], showing the importance of preserving the three-dimensional sp^3 Cd-Se network. To optimize the core-cage structures [$(\text{CdSe})_{12+1=13}$, $(\text{CdSe})_{28+5=33}$, and $(\text{CdSe})_{28+6=34}$] we created different starting arrangements assuming different orientations for the encapsulated $\text{CdSe}_{n=1,5,6}$ units.¹⁷ In the relaxed assemblies the

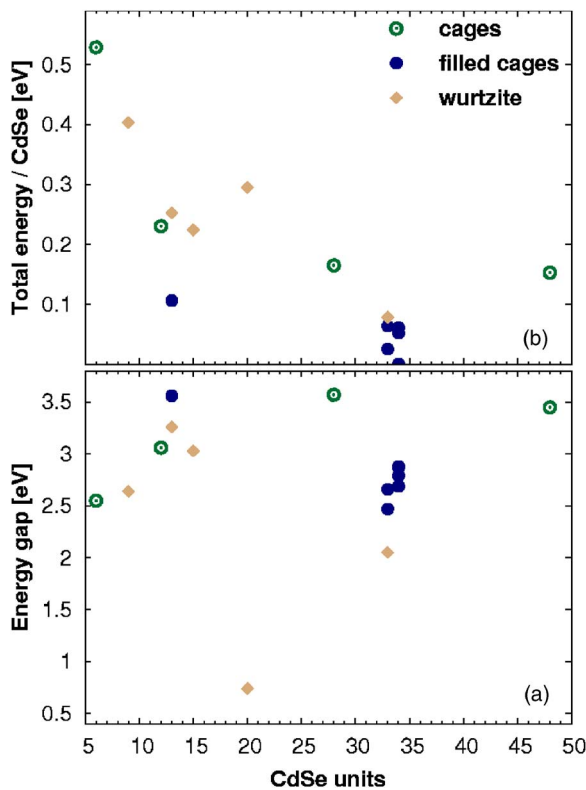


FIG. 3. (Color online) Calculated total energies per CdSe unit (a) and HOMO-LUMO gaps (b) as a function of the number of CdSe units. The zero of energy is set to the total energy per pair of the $(\text{CdSe})_{34}$ core-cage. The empty (filled) circles refer to cage (core-cage) clusters, while the diamonds refer to wurtzite-based structures.

distributions of bond lengths and angles result very similar despite of the distinct initial configurations. Nevertheless, we decided to use few distinguishable relaxed geometries in the spectroscopy calculations in order to evaluate the dependence of the optical spectra on small changes in the atomic positions.

In Fig. 3(a) we summarize our results for the total energy per CdSe unit in the configurations studied here. The zero of energy is set to the lowest energy structure of $(\text{CdSe})_{34}$. The core-cage $(\text{CdSe})_{33}$ cluster is significantly more deformed under optimization than $(\text{CdSe})_{34}$, but it turns out to have a very similar binding energy. We thus confirm that the fullerene-like geometries are particularly stable.¹¹ The filled cage structure made of 13 units gives as well a relative minimum in the total energy per pair. In the case of $(\text{CdSe})_{13}$ and $(\text{CdSe})_{33}$ it is possible to compare the total energies of the different three-dimensional isomers: the core-cage nanoparticles have a slightly higher binding energy [0.15 eV for $(\text{CdSe})_{13}$ and 0.05 eV for $(\text{CdSe})_{33}$]. However, we should not forget that the energy differences we are discussing here are all very tiny, sometimes of the same order of magnitude as the accuracy of the calculations. That fact confirms how difficult it can be to extract structural information from a single number (the total energy) and leads to the conclusion that the simple analysis of total energy differences cannot be conclusive to demonstrate the existence of fullerene-like CdSe clusters.

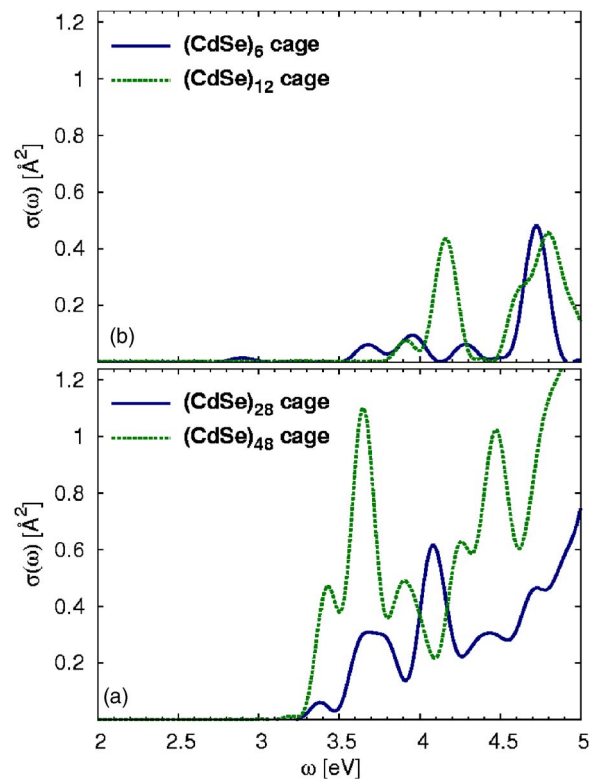


FIG. 4. (Color online) Photoabsorption cross section $\sigma(\omega)$ of the empty cages. In panel (a) the absorption spectra of $(\text{CdSe})_{48}$ (dotted line) and $(\text{CdSe})_{28}$ (solid line); in panel (b) the absorption spectra of $(\text{CdSe})_{12}$ (dotted line) and $(\text{CdSe})_6$ (solid line).

III. OPTICAL ABSORPTION

From the relaxed geometries we obtain the optical spectra at zero temperature using time-dependent density functional theory (TDDFT)¹⁸ in the adiabatic local density approximation.¹⁹ Of course, calculations can be predictive only if the theoretical approach employed guarantees a precise assignment of the peak positions. *Ab initio* spectroscopy calculations in TDDFT have already proved to be a reliable and efficient tool to characterize structural transitions in C and B clusters.^{20,21} In the same implementation²² used here, TDDFT has been applied to study metal and semiconducting clusters,^{21,23} aromatic molecules,²⁴ protein chromophores,²⁵ etc., reproducing the low energy peaks of the optical spectra with an average accuracy below 0.2 eV.²³ The accuracy in reproducing transitions of intermediate energy is known to be somewhat deteriorated, due to the wrong asymptotic behavior of the LDA exchange-correlation potential. For this reason, we will focus the analysis of our results on the lowest energy peaks.

In Fig. 4 we display the photoabsorption spectra of the empty cages of different diameters. First of all, we observe that the absorption threshold is systematically blueshifted with respect to the bulk optical gap (≈ 1.8 eV). In particular, due to quantum confinement effects, the shift is more pronounced when the cluster size is smaller. Second, we can compare the absorption threshold with the Kohn-Sham gap between the HOMO-LUMO reported in Fig. 3(a): the Kohn-

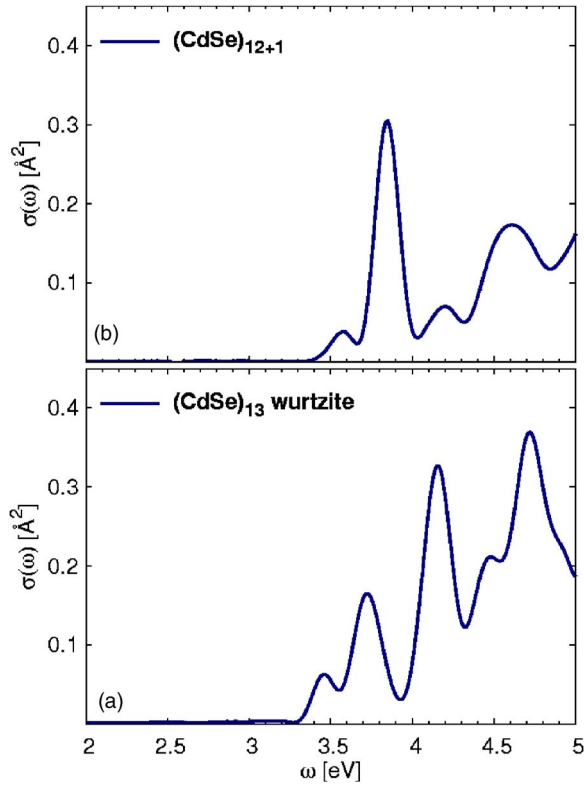


FIG. 5. (Color online) Photoabsorption cross section $\sigma(\omega)$ of the isomers of $(\text{CdSe})_{13}$. In panel (a) the absorption spectrum of the wurtzite structure; in panel (b) the absorption spectrum of the filled cage.

Sham gap is systematically smaller than the TDDFT absorption threshold. It is well known that the simpler approach of taking the differences of eigenvalues between HOMO and LUMO orbitals gives peaks at lower frequencies in complete disagreement with the experimental spectra.²⁰ We note that the TDDFT optical gaps include both electron-electron and electron-hole corrections to the Kohn-Sham gap at the level of the adiabatic local density approximation.

We should keep in mind that the opening of the gap due to confinement can be counterbalanced by a closing of the gap due to surface reconstruction. This leads to a nontrivial dependence of the absorption gap as a function of the cluster size. This effect is already present at the Kohn-Sham level [see Fig. 3(a)] and it persists in TDDFT spectra. In fact, the calculated absorption curves are strongly dependent not only on the cluster size but also on the details of its atomic arrangement. This is evident if we compare the optical response of the different isomers of $(\text{CdSe})_{13}$ in Fig. 5 and of $(\text{CdSe})_{33}$ in Fig. 6. The absorption threshold is lower in wurtzite-type clusters as the HOMO-LUMO gap is reduced due to the presence of defect states in the gap as a consequence of the strong surface deformation. For a similar reason, the larger surface deformation of the core-cage $(\text{CdSe})_{33}$ aggregate in comparison with the more stable $(\text{CdSe})_{34}$ structure explains why the first starts absorbing at lower energies than the second. Finally, we note that the similar curves of different colors in panels (c) and (d) of Fig. 6 correspond to distinct core-cage geometries obtained in various optimiza-

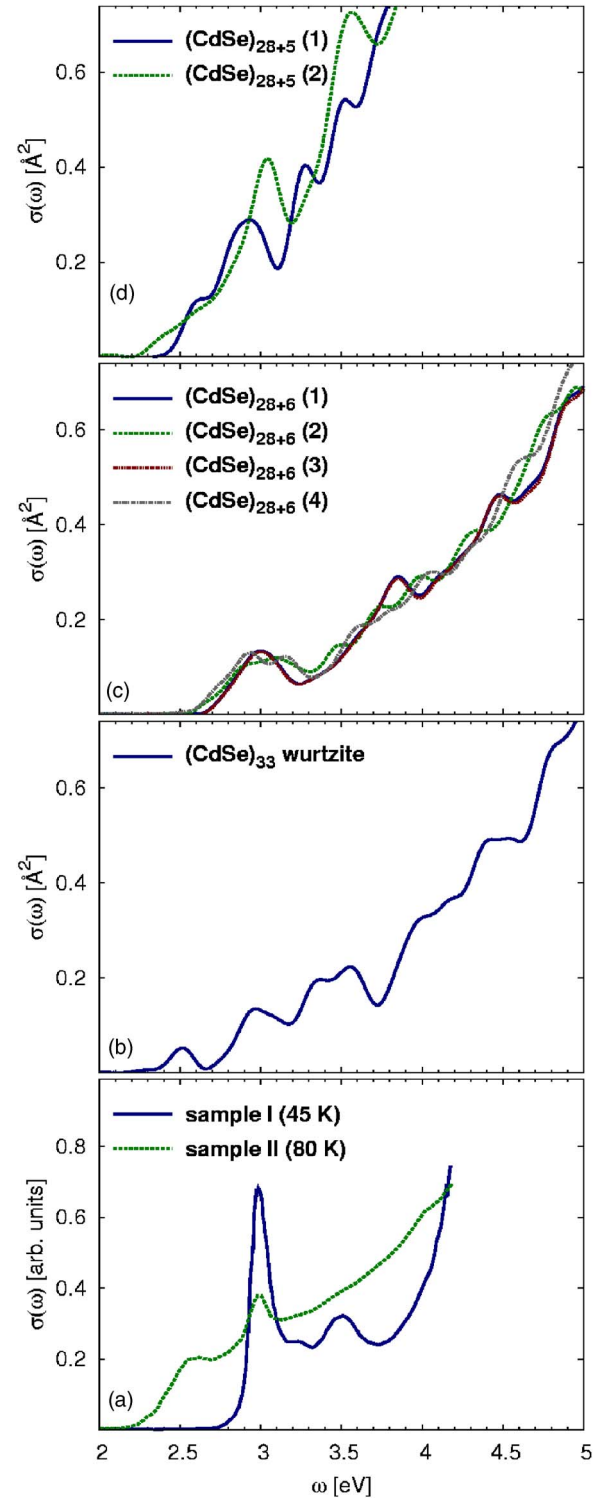


FIG. 6. (Color online) Photoabsorption cross section $\sigma(\omega)$ of the isomers of $(\text{CdSe})_{33,34}$. The experimental data in arbitrary units (a) are compared with our calculated spectra (b), (c), and (d). The different curves in panels (c) and (d) correspond to distinct relaxed geometries obtained starting from different filled cages.

tion simulations. We conclude that the dependence of the relevant peak positions and shapes on the different atomic arrangements is not negligible, but the peak positions and oscillator strengths are sufficiently defined for our purposes.

A comparison with measured spectra¹¹ is possible for nanoparticles made of 33 and 34 CdSe units (see Fig. 6). The solid blue line in panel (a) of Fig. 6 refers to room temperature absorption data for mass-selected nanoparticles prepared in toluene at 45 °C (sample I), while the green dotted line correspond to analogous data for the solution prepared at 80 °C (sample II). Both samples are characterized by strong absorption at 3 eV. For sample II the experimental data show the appearance of a broad peak extending to lower energies. This peak turns out to move to even lower energies when the temperature and the time in the synthesis process increase. In a simple quantum confinement picture, these findings suggest that larger particles, possibly reconstructed bulk fragments, are formed when the temperature increases. Moreover, the sharp peak at about 3 eV, which is always present, was hypothesized to be the signature of the highly resistant fullerene-like clusters.

Our calculated spectra shown in Fig. 6 prove the presence of fullerene-like core-cage structures. The theoretical optical response of all our model core-cage (CdSe)₃₄ clusters is indeed characterized by a well-defined absorption peak at 3 eV. Also the core-cage (CdSe)₃₃ cluster and the (CdSe)₃₃ reconstructed bulk fragment can contribute to this peak. However, they cannot be present in sample I, as that would be signaled by the appearance of a broader peak at lower energy, which is absent in the experimental spectrum. On the other hand, a peak at about 2.5 eV, connected to the peak at 3 eV by a region of increasing absorption, is present in the spectrum for sample II. Our calculations show that the (CdSe)₃₃ wurtzite fragment is responsible for the peak at 2.5 eV, while the broad absorption region between 2.5 and 3 eV can be explained by the presence of (CdSe)₃₃ core-cage structures. This is in disagreement with the intuition of Ref. 11 that bulk fragments of about 2.0 nm gave rise to the broad absorption below 3 eV. Although it is true that a peak in that energy range is typical of 2.0 nm crystalline-like TOPO-passivated nanoparticles,² the effect of the structural deformation of ligand-free samples is more than a simple broadening of the absorption line. In fact, ligand-free cluster can absorb at lower energies than passivated cluster of the same

size due to a closing of the gap induced by surface reconstruction. On the other hand, the experimental evidence of a continuous redshift of the 2.5 eV peak when the temperature and the time of the synthesis process increase can only be explained by the gradual addition of atoms to the (CdSe)₃₃ bulk fragment, as the creation of the next stable core-cage structure would require filling the successive fullerene-like cage made of 48 CdSe units.

IV. CONCLUSIONS

In summary, we performed an *ab initio* study of CdSe nanoparticles, considering different cluster sizes and atomic arrangements. Upon geometry optimization, these clusters get slightly contracted and puckered, with Cd atoms pulled in and Se atoms pushed out. The most stable structures were, as expected from previous results, fullerene-like clusters including a wurtzite core. Optical spectra calculated with TD-DFT turn out to be blue-shifted with respect to the bulk gap, due to confinement effects, and red-shifted with respect to the Kohn-Sham HOMO-LUMO gaps, due to the inclusion of electron-electron and electron-hole interactions at the level of the adiabatic LDA. As the opening of the gap due to confinement can be counterbalanced by a closing of the gap due to surface reconstruction, we found a nontrivial dependence of the absorption gap as a function of the cluster size. Furthermore, by comparing our theoretical spectra with measurements, we could prove the existence of the stable core-cage fullerene-like structures recently hypothesized.

ACKNOWLEDGMENTS

We would like to thank A. Rubio for many useful discussion. We further acknowledge partial support by the EC Network of Excellence NANOQUANTA (NMP4-CT-2004-500198). Computations were performed at the Institut du Développement et des Ressources en Informatique Scientifique (IDRIS, France, project #020544) and at the Laboratório de Computação Avançada of the University of Coimbra (Portugal).

¹M. G. Bawendi, M. L. Stiegerwald, and L. E. Brus, *Annu. Rev. Phys. Chem.* **41**, 477 (1990).

²C. B. Murray, D. J. Norris, and M. G. Bawendi, *J. Am. Chem. Soc.* **115**, 8706 (1993).

³S. Coe, W. K. Woo, M. G. Bawendi, and V. Bulovic, *Nature (London)* **420**, 800 (2002).

⁴N. Tessler, V. Medvedev, M. Kazes, S. H. Kan, and U. Banin, *Science* **295**, 1506 (2002).

⁵V. I. Klimov, *Los Alamos Sci.* **28**, 214 (2003); N. C. Greenham, X. Peng, and A. P. Alivisatos, *Phys. Rev. B* **54**, 17628 (1996).

⁶M. T. Harrison, S. V. Kershaw, M. G. Burt, A. L. Rogach, A. Kornowski, A. Eychmüller, and H. Weller, *Pure Appl. Chem.* **72**, 295 (2000).

⁷M. Bruchez, M. Moronne, P. Gin, S. Weiss, and A. P. Alivisatos, *Science* **281**, 2013 (1998); X. Michalet, F. F. Pinaud, L. A.

Bentolila, J. M. Tsay, S. Doose, J. J. Li, G. Sundaresan, A. M. Wu, S. S. Gambhir, and S. Weiss, *ibid.* **307**, 538 (2005).

⁸J. J. Shiang, A. V. Kadavanich, R. K. Grubbs, and A. P. Alivisatos, *J. Phys. Chem.* **99**, 17417 (1995).

⁹E. Rabani, *J. Chem. Phys.* **115**, 1493 (2001).

¹⁰A. Puzder, A. J. Williamson, F. Gygi, and G. Galli, *Phys. Rev. Lett.* **92**, 217401 (2004).

¹¹A. Kasuya, R. Sivamohan, Y. A. Barnakov, I. M. Dmitruk, T. Nirasawa, V. R. Romanyuk, V. Kumar, S. V. Mamykin, K. Tohji, B. Jeyadevan, K. Shinoda, T. Kudo, O. Terasaki, Z. Liu, R. V. Belosludov, V. Sundararajan, and Y. Kawazoe, *Nat. Mater.* **3**, 99 (2004).

¹²A. Kasuya, Y. Noda, I. Dmitruk, V. Romanyuk, Y. Barnakov, K. Tohji, V. Kumar, R. Belosludov, Y. Kawazoe, and N. Ohuchi, *Eur. Phys. J. D* **34**, 39 (2005).

- ¹³J. M. Soler, E. Artacho, J. D. Gale, A. García, J. Junquera, P. Ordejón, and D. Sánchez-Portal, *J. Phys.: Condens. Matter* **14**, 2745 (2002).
- ¹⁴N. Troullier and J. L. Martins *Phys. Rev. B* **43**, 1993 (1991).
- ¹⁵J. P. Perdew and A. Zunger, *Phys. Rev. B* **23**, 5048 (1981).
- ¹⁶J.-Y. Zhang, X.-Y. Wang, M. Xiao, L. Qu, and X. Peng, *Appl. Phys. Lett.* **81**, 2076 (2002).
- ¹⁷See EPAPS Document No. E-PRBMDO-74-100647 for images of the structures shown in Fig. 1. For more information on EPAPS, see <http://www.aip.org/pubserve/epaps.html>.
- ¹⁸E. Runge and E. K. U. Gross, *Phys. Rev. Lett.* **52**, 997 (1984); *Time-Dependent Density Functional Theory*, edited by M. A. L. Marques, C. Ullrich, F. Nogueira, A. Rubio, K. Burke, and E. K. U. Gross, *Lecture Notes in Physics*, Vol. 706 (Springer, Berlin, 2006).
- ¹⁹E. K. U. Gross and W. Kohn, *Phys. Rev. Lett.* **55**, 2850 (1985); *Phys. Rev. Lett.* **57**, 923 (1986).
- ²⁰A. Castro, M. A. L. Marques, J. A. Alonso, G. F. Bertsch, K. Yabana, and A. Rubio, *J. Chem. Phys.* **116**, 1930 (2002).
- ²¹M. A. L. Marques and S. Botti, *J. Chem. Phys.* **123**, 014310 (2005).
- ²²M. A. L. Marques, A. Castro, G. F. Bertsch, and A. Rubio, *Comput. Phys. Commun.* **151**, 60 (2003); A. Castro, H. Appel, M. Oliveira, C. A. Rozzi, X. Andrade, F. Lorenzen, M. A. L. Marques, E. K. U. Gross, and A. Rubio, *Phys. Status Solidi B* **243**, 2465 (2006); the code octopus is available at <http://www.tddft.org/programs/octopus/>.
- ²³A. Castro, M. A. L. Marques, J. A. Alonso, and A. Rubio, *J. Comput. Theor. Nanosci.* **1**, 231 (2004).
- ²⁴K. Yabana and G. F. Bertsch, *Int. J. Quantum Chem.* **75**, 55 (1999); G. Mallocci, G. Mulas, and C. Joblan, *Astron. Astrophys.* **426**, 105 (2004).
- ²⁵M. A. L. Marques, X. Lopez, D. Varsano, A. Castro, and A. Rubio, *Phys. Rev. Lett.* **90**, 258101 (2003).